

# Nuclear Spin-Kinetics of $^3\text{He}$ in Carbonizates with Various Porosity

M.S. Tagirov · A.N. Yudin · G.V. Mamin ·  
A.A. Rodionov · D.A. Tayurskii · A.V. Klochkov ·  
R.L. Belford · P.J. Ceroke · B. M. Odintsov

Published online: 21 June 2007  
© Springer Science+Business Media, LLC 2007

**Abstract** In the present work the NMR relaxation of the gaseous  $^3\text{He}$  inside carbonizate pores was investigated at temperature 1.5 K. The carbonizates synthesized from fructose and wood of the tropical tree astronium were used. The dependences of the  $^3\text{He}$  relaxation rates  $T_1$  and  $T_2$  on the gas pressure and the amount of the  $^3\text{He}$  atoms adsorbed on the surface of pore walls were measured. The analysis of obtained results reveals the existence of the  $^3\text{He}$  phases inside carbonizate—adsorbed solid layers, liquid and gas.

## 1 Introduction

The system “Carbonizate– $^3\text{He}$ ” was studied for the nuclear dynamic polarization (DNP) method for the  $^3\text{He}$  nuclei to be developed [1, 2]. Activated charcoals with large surface and a lot of surface paramagnetic centers can be used in such experiments. As an activated charcoal the carbonizate made of fructose was studied [2]. But this type of carbonizate had a lot of  $^1\text{H}$  nuclei impurities, localized near the surface paramagnetic centers. These impurities create a spin–polarization leakage channel. Fructose carbonizate cleaning is difficult, wood carbonizates are more appropriate from this point of view.

---

M.S. Tagirov (✉) · A.N. Yudin · G.V. Mamin · A.A. Rodionov · D.A. Tayurskii · A.V. Klochkov  
Kazan State University, 420008 Kazan, Russia  
e-mail: Murat.Tagirov@ksu.ru

R.L. Belford · P.J. Ceroke · B. M. Odintsov  
Illinois Research EPR center, University of Illinois, Urbana, IL 61801, USA

B. M. Odintsov  
Institute of Radio Engineering and Electronics RAS, 125009 Moscow, Russia

## 2 Carbonizate Properties

Samples of carbonized wood were synthesized at temperatures of  $580\div 750^\circ\text{C}$  from wood of the tropical tree astronium from Central America. The precursor was carbonized under  $\text{CH}_4$  or  $\text{H}_2$  flow in a special computer-controlled programmable multizone furnace [3]. After steam processing, grinding and sizing the set of calibrated samples was obtained. Fructose sample was carbonized in the same way under  $\text{NH}_3$  flow.

The samples were studied by scanning electron microscope (Philips XL30 ESEM). It follows from Fig. 1 that in astronium carbonizate possesses many “narrow-channel” like pores (size of about  $5\ \mu\text{m}$ ), while fructose carbonizate sample looks quite different. When the particles size becomes less than  $10\ \mu\text{m}$ , the porous structure of astronium carbonizate is destroyed. The NMR-cryoporometry data show, that there are fine pores with size less than  $10\ \text{nm}$  in the samples, as well. It should be emphasized that temperature pyrolysis can result in formation of very fine micropores [4].

The EPR measurements showed, that properties of paramagnetic centers in fructose [5] and in astronium carbonizates are similar. The majority of paramagnetic centers are distributed on the carbonizate surface [6]. The paramagnetic centers concentration was about 10–50% of surface atoms, and astronium carbonizate with particles

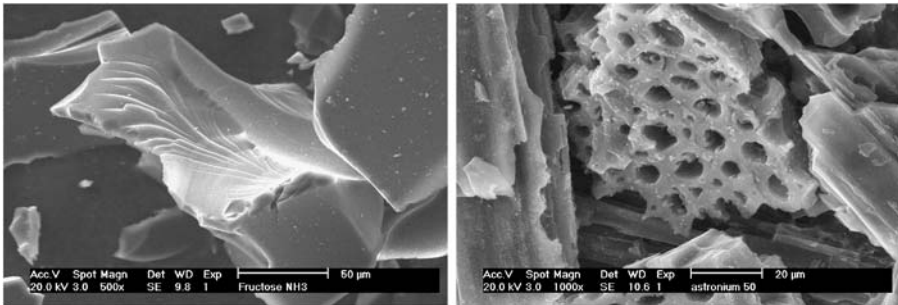
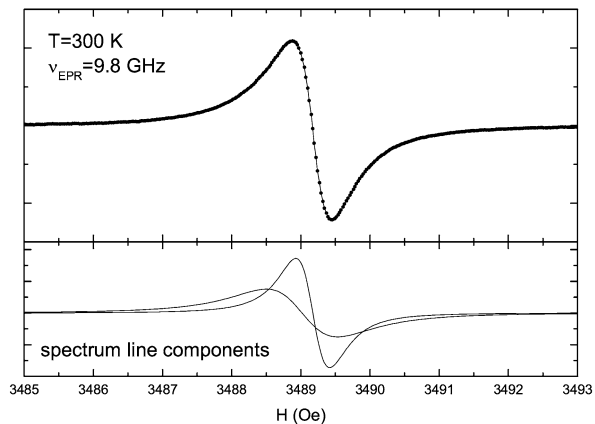


**Fig. 1** Photo of fructose carbonizate and astronium wood carbonizate (particles size  $50\text{--}75\ \mu\text{m}$ )

**Fig. 2** EPR line in astronium carbonizate. The two Lorentzian lines used for approximation are shown as well



size 50–75 μm had a higher paramagnetic centers concentration. The EPR line was well approximated by two Lorentzians (Fig. 2). We suppose that narrow part corresponds to the paramagnetic centers that appeared during carbonization and wide part can be attributed to the centers that appeared during grinding procedure.

### 3 Methods

For <sup>3</sup>He NMR-relaxation measurements the pulse NMR spectrometer with frequency range 2–20 MHz was used. Spin–lattice relaxation time  $T_1$  was measured by observation of spin–echo recovery after saturating pulse. Spin–spin relaxation time  $T_2$  was measured by Hahn method. Transverse magnetization decay in astronium was well approximated with single exponential function. This indicates, that <sup>3</sup>He nuclei diffusion in inhomogeneous magnetic field does not influence on the <sup>3</sup>He relaxation, because experiment time  $2\tau$  is much longer than <sup>3</sup>He molecule flight time between carbonate walls.

### 4 Results

The nuclear spin–lattice ( $T_1^{-1}$ ) and the spin–spin ( $T_2^{-1}$ ) relaxation rates of <sup>3</sup>He were measured at temperature 1.5 K and at different pressures [7]. Three phases in the experiment were presented: solid <sup>3</sup>He layers, gaseous <sup>3</sup>He and liquid <sup>3</sup>He. At the beginning, during gas injection into the system all the gas molecules were adsorbed by carbonate surface, so measured pressure was almost zero. After adsorption capacity was reached, new portions of <sup>3</sup>He gas filled the volume of cell. When condensation point achieved (saturation vapor pressure is 50.3 Torr at  $T = 1.5$  K) [8], liquid <sup>3</sup>He phase appears, the pressure stays constant.

We could not measure directly a precise quantity of helium in the system, so it was estimated using <sup>3</sup>He nuclear magnetization value ( $M_{z0}$ ), determined by using NMR (from intensity of spin echo). Dependences of  $T_1^{-1}$  and  $T_2^{-1}$  on nuclear magnetization are shown on the Fig. 3 (1 a.u. corresponds about  $10^{17}$  of <sup>3</sup>He atoms). As

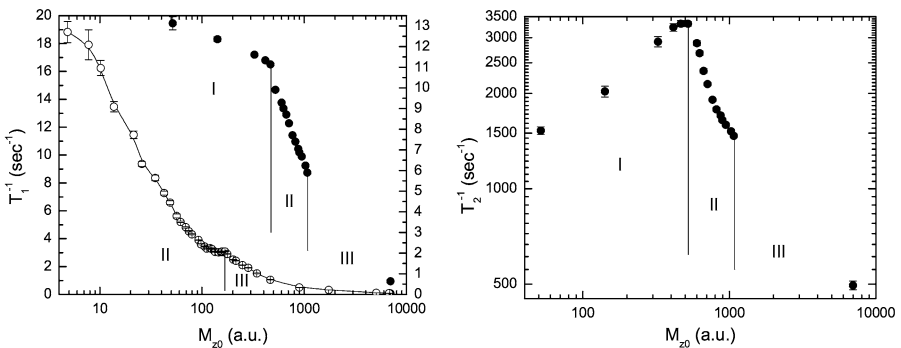


**Fig. 3** Nuclear <sup>3</sup>He spin–lattice ( $T_1^{-1}$ ) and spin–spin ( $T_2^{-1}$ ) relaxation rates dependence on helium nuclei quantity (○—fructose, ●—astronium)

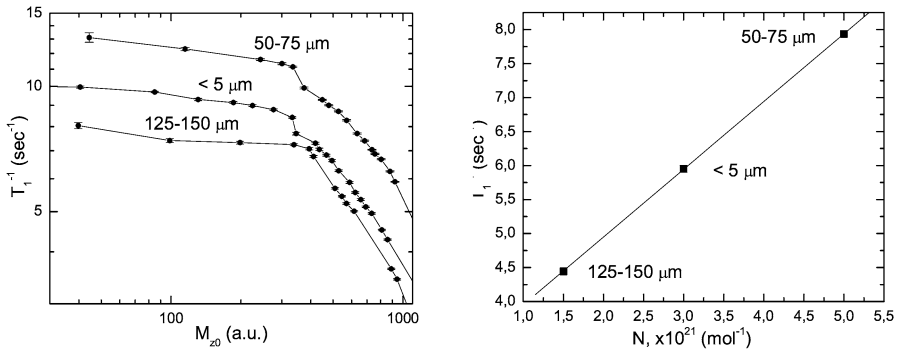


**Fig. 4**  $^3\text{He}$  nuclear spin–lattice relaxation rates dependences on helium nuclei quantity and on paramagnetic centers concentration (the pressure of  $^3\text{He}$  was 20 Torr) in astronium carbonizates with different sizes

shown, during adsorption (range I)  $T_1^{-1}$  rate changes slowly and  $T_2^{-1}$  increases by a factor of more than two. At  $M_{20} \approx 500$  a.u. (that corresponds  $5 \cdot 10^{19}$  of  $^3\text{He}$  atoms per 77 mg of carbonizate and is determined by adsorption capacity of carbonizate) gaseous phase appears (pressure is not zero, range II) and the slope of the dependences changes. The  $T_1^{-1}$  rate decreases exponentially and the  $T_2^{-1}$  slows down after maximum.

The results of measuring  $T_1^{-1}$  ( $\circ$ ) in fructose carbonizate are presented on the same figure for comparison. Surface structure of fructose carbonizate is not developed and adsorbability is less, so it was impossible to study zero pressure range, which corresponds to filling surface by adsorbing helium nuclei. But when the pressure is not equal to zero, the  $T_1^{-1}$  rate change is more rapid than in astronium.

The described measurements were made with astronium samples which had different size of particles (<5  $\mu\text{m}$ , 50–75  $\mu\text{m}$  and 125–150  $\mu\text{m}$ ). The  $T_1^{-1}$  of  $^3\text{He}$  dependences (Fig. 4) were similar for all samples, but the spin–lattice relaxation was more rapid for the sample 50–75  $\mu\text{m}$ . This fact seems to be strange, but mentioned above data of EPR measurements can explain this result. The different samples of astronium carbonizate had the different concentration of surface paramagnetic centers and we can depict the dependence of nuclear  $^3\text{He}$  spin–lattice ( $T_1^{-1}$ ) relaxation rates on paramagnetic centers concentration (Fig. 4). One can see, the longitudinal relaxation rate  $^3\text{He}$  is linearly proportional with concentration of paramagnetic centers.

## 5 Discussion

As the  $^3\text{He}$  nuclear spin–lattice relaxation rate depended on concentration of paramagnetic centers (Fig. 4), and the rate was rather rapid, we could conclude that the main channel of spin–lattice relaxation was determined by the surface paramagnetic centers. The magnetic capacity of paramagnetic system was not too high, so relaxation of large quantity of nuclei through paramagnetic centers could be limited.

At the region I all atoms of  $^3\text{He}$  are adsorbed by the carbonizate and situated near the paramagnetic centers so there is the most rapid spin–lattice relaxation. At

the region II the gaseous  $^3\text{He}$  appears. There is rather intensive exchange between gaseous phase and adsorbed layers of  $^3\text{He}$  and rapid self-diffusion, so the  $T_1^{-1}$  rate is averaged. But while the pressure and magnetic capacity of nuclear spin system grow, the relaxation channel stays the same. So the relaxation rate rapidly decreases at the regions II and III.

Rate  $T_2^{-1}$  is proportional to homogeneous NMR line width of  $^3\text{He}$ , so it depends mostly on the distance between spins. In the range I where the carbonizate surface adsorbs  $^3\text{He}$  atoms, the distance becomes smaller and  $T_2^{-1}$  increases. In the ranges II and III there are atoms with large distance between them. So the more gaseous  $^3\text{He}$  present in the system the smaller  $T_2^{-1}$  becomes.

## 6 Conclusion

The wood carbonizates are characterized by the well-developed surface and high concentration of paramagnetic centers on it. That is why these carbonizates are more appropriate to realize dynamic nuclear polarization than fructose carbonizates or other. Astronium wood carbonizate represents an unique model system to study phase change and to determine phase change influence on spin kinetics of quantum liquids, like  $^3\text{He}$ .

**Acknowledgements** This research is partly supported by Russian Foundation for Basic Research (grant # 06-02-17241).

## References

1. L.W. Engel, K. DeConde, *Phys. Rev. B* **33**, 2035 (1986)
2. G.V. Mamin, H. Suzuki, M.S. Tagirov, D.A. Tayurskii, A.N. Yudin, *JETP Lett.* **79**, 641 (2004)
3. R.B. Clarkson, B.M. Odintsov, P.J. Ceroke, J.H. Ardenkjær-Larsen, M. Fruianu, R.L. Belford, *Phys. Med. Biol.* **43**, 1907 (1998)
4. R.S. Vartapetyan, A.M. Voloshchuk, A.K. Buryak, C.D. Artamonova, R.L. Belford, P.J. Ceroke, D.V. Kholine, R.B. Clarkson, B.M. Odintsov, *Carbon* **43**, 2152 (2005)
5. G.V. Mamin, H. Suzuki, M.S. Tagirov, V.N. Efimov, A.N. Yudin, *Phys. B* **329–333**, 1237 (2003)
6. V.A. Atsarkin, G.A. Vasneva, V.V. Demidov, F.S. Dzheparov, B.M. Odintsov, R.B. Clarkson, *JETP Lett.* **72**, 369 (2000)
7. G.V. Mamin, M.S. Tagirov, D.A. Tayurskii, A.N. Yudin, R.L. Belford, P.J. Ceroke, B.M. Odintsov, *JETP Lett.* **84**, 41 (2006)
8. B.M. Abraham, D.W. Osborne, B. Weinstock, *Phys. Rev.* **80**, 366 (1950)